

PERFORMANCE ENHANCEMENT OF INDIRECT MATRIX CONVERTER FED BLDC MOTOR USING FIREFLY ALGORITHM

Subha Karuvelam

Government College of Engineering, Tirunelveli, Tamilnadu, India.

subha@gcetly.ac.in

Abstract - This paper presents firefly algorithm (FFA) based optimal gain tuning of PI speed and torque/current controllers in an indirect matrix converter (IMC) fed brushless DC motor (BLDC). Optimization considers variation in speed and load torque, and provides appropriate gains to PI speed and PI torque controller to obtain the better dynamic and steady state response and enhancement of input current. The performance of the BLDC motor is checked with the gains from Ziegler-Nichols tuning method and FFA based tuning through the MATLAB Simulink. The results of both the systems are compared. From the simulation results based on time domain analysis, it is proved that the gains of PI speed and PI torque controller using FFA performs better than that of Ziegler-Nichols tuning method. The simulation results are validated using the experimental setup.

Keywords - Indirect Matrix Converter, Brushless DC motor, Firefly Algorithm, PI Controller

I INTRODUCTION

The torque ripple produces undesirable variation in speed and inaccuracy in motion control in low speed of operation whereas in high speed, the motor inertia itself filters out the torque ripple. The torque ripple in BLDC can be minimized either by the control techniques or by improving motor design. The motor design includes skewing of slots, fractional slot winding, short-pitch winding, increased number of phases, air gap windings, adjusting stator slot opening and wedges, design in rotor magnet pole arc, its position and width. The control technique in minimization of torque ripple involves adaptive control technique, pre-programmed current waveform control, selective harmonic injection technique, estimators and observers, speed loop disturbance rejection, high speed current regulators, commutation torque minimizations and automated self-commissioning schemes etc.

In [1], an adaptive observer was designed to estimate the torque ripple and the estimated torque ripple was injected to cancel out the disturbance in torque. In [2], ILC in time domain and modified ILC in frequency domain were used to reduce the torque ripple in PMSM. Buck converter, super lift Luo converter and SEPIC were used to adjust the DC bus voltage which reduces the torque ripple in brushless motors [3] – [5]. For the motor with non-ideal back EMF, direct torque control method, motor back EMF waveform function and PWM-ON-PWM methods were used to regulate the current which reduce the torque ripple, whereas for the motor with ideal back EMF, PWM ON pattern was used [6] – [7]. In the back EMF waveform function method, the higher order harmonics of back EMF were neglected due to the time consuming calculation. Direct self-control method for the torque ripple minimization was proposed in [8] where the trivector stator voltage and flux are projected in X-Y plane of 3D space. From which the periodic change of stator flux with respect to the rotor position was derived and controlled which reduce the torque ripple. In the small inductance BLDC motor, the torque ripple was reduced by compensating the back EMF disturbance by feed forward control, compensating the problem of unbalancing of three phase winding by asymmetric compensation function and using DC link buck converter PWM control method [9] – [10].

These approaches are theoretically complex and difficult to implement. The conventional PID controller offers solution to most of the real world application in terms of better steady state and dynamic response. But tuning the gains of PID controller is quite difficult. Due to the high performance requirement of the modern industry, computational intelligence techniques are proposed for optimal tuning of the gains [11]. In [11] and [12], the authors used particle swarm optimization and bacterial foraging for tuning the parameters of PID controller.

In this paper, a robust PI current/torque controller and PI speed controller are designed. Firefly algorithm (FFA) is proposed to tune the gains of PI controllers for reducing the overshoot in speed response and torque ripple and to improve the input current of the BLDC motor. The proposed approach is compared with the Ziegler-Nichols tuning method.

II INDIRECT MATRIX CONVERTER

Matrix converters are classified into direct matrix converter (DMC) and indirect matrix converter (IMC). Direct matrix converter consists of nine bidirectional switches arranged in matrix form that allows any load phase to be connected to any source phase directly. The indirect matrix converter has current source rectifier (CSR) at the input side, a voltage source inverter (VSI) at the load side and a fictitious DC link without energy storage element. Fig. 1 shows the circuit diagram of IMC. The synchronization of the modulation process of CSR and VSI is necessary due to the absence of DC storage element. In [13], [14], the authors proposed different types of IMC which differ in CSR topology and mainly affects the direction of power flow.

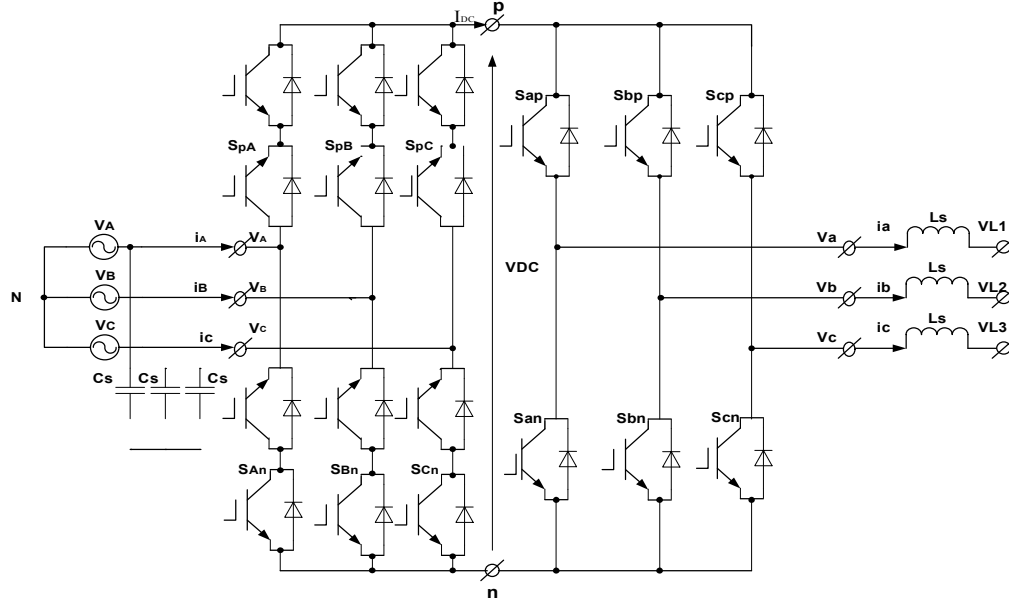


Figure 1. Indirect Matrix Converter

The DMC performs AC/AC conversion in single stage whereas IMC performs in two stages namely rectification using CSR and inversion using VSI. Hence control of IMC is easier compared to the DMC. In [15], the author proposed DTC to reduce the torque ripple of IMC fed induction motor.

2.1 Current Source Rectifier

The modulation strategy of the CSR is as same as the conventional modulation strategy of the conventional rectifier. The purpose of the modulation in the CSR is to produce maximum voltage in the DC link and to maintain the sinusoidal and balanced input current with controllable displacement angle with respect to the input voltage. The rectifier stage synthesizes a positive voltage of the DC link by selecting a switching state. Due to the inductive nature of the load, the output current i_p is assumed constant for each switching period. Hence the load of the rectifier is assumed to be constant DC current sink with the current $i_p = I_{DC}$. In this paper space vector modulation (SVM) technique is used for CSR. In SVM, the input current is transformed into six distinctive input space vectors. The vector diagram is shown in figure 2. The magnitude of these current vectors depends on the instantaneous value of the current i_p . The switching sequences of CSR is shown in Table 1. The CSR is modulated to supply the maximum DC link voltage to improve the voltage transfer ratio. Hence always the modulation index m_R is set to unity. As a result, the zero current vector in the rectification stage is eliminated and contains only two vectors I_α and I_β . The duty cycles, DC link voltage and DC link current are given as

$$d_\alpha = \sin\left(\frac{\pi}{3} - \theta_i\right) \& d_\beta = \sin \theta_i$$

$$V_{PN} = d_\alpha^R V_{I\alpha} + d_\beta^R V_{I\beta} \& i_p = d_\alpha i_\alpha + d_\beta i_\beta$$

Table 1. Switching Sequences of CSR

Switching State						DC link voltages			Input currents		
S_{pA}	S_{pB}	S_{pC}	S_{An}	S_{Bn}	S_{Cn}	V_p	V_n	V_{pn}	i_A	i_B	i_C
1	0	0	0	0	1	V_A	V_C	V_{AC}	i_p	0	$-i_p$
0	1	0	0	0	1	V_B	V_C	V_{BC}	0	i_p	$-i_p$

0	1	0	1	0	0	V_B	V_A	V_{BA}	$-i_p$	i_p	0
0	0	1	1	0	0	V_C	V_A	V_{CA}	$-i_p$	0	i_p
0	0	1	0	1	0	V_C	V_B	V_{CB}	0	$-i_p$	i_p
1	0	0	0	1	0	V_A	V_B	V_{AB}	i_p	$-i_p$	0
1	0	0	1	0	0	V_A	V_A	0	0	0	0
0	1	0	0	1	0	V_B	V_B	0	0	0	0
0	0	1	0	0	1	V_C	V_C	0	0	0	0

2.2 Voltage Source Inverter

The function of the VSI is to excite the BLDC motor stator winding according to the rotor position so as to synchronize the stator rotating magnetic field with the rotating permanent magnetic field. The rotor position of the motor is obtained from three hall sensors. Since 180° magnetic arc BLDC motor is used, 120° conduction interval is applied to the VSI to maintain the stator current as rectangular so as to produce the constant torque. In 120° conducting interval, only two devices are in ON state. The inverter is commutated at every 60 electrical degrees so that the rectangular line current is in phase with the back EMF. The switching sequence of VSI is shown in table 2.

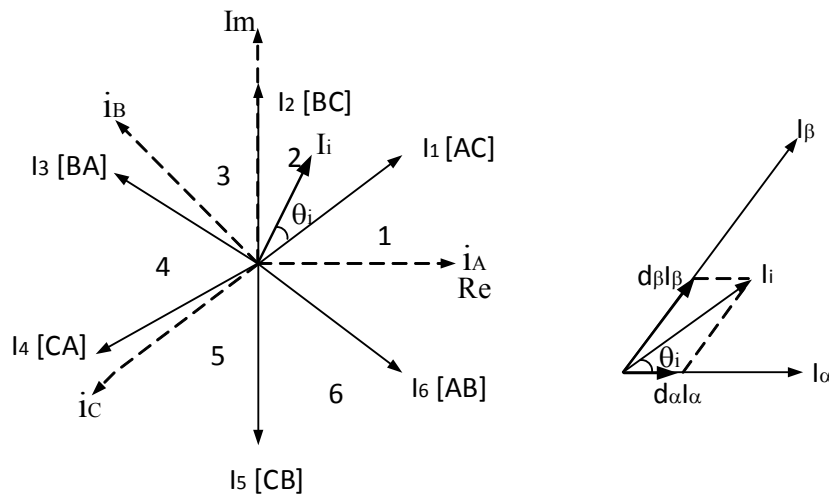


Figure 2. Vector diagram

Table 2. Switching sequence of VSI

Rotor Position	Forward Rotation						ON state switches
	Hall Sensor Output			Output Phase			
	H1	H2	H3	a	b	c	
0 - 60°	1	0	0	1	0	-1	$S_{ap} \& S_{cn}$
60 - 120°	1	0	1	1	-1	0	$S_{ap} \& S_{bn}$
120 - 180°	0	0	1	0	-1	1	$S_{cp} \& S_{bn}$
180 - 240°	0	1	1	-1	0	1	$S_{cp} \& S_{an}$
240 - 300°	0	1	0	-1	1	0	$S_{bp} \& S_{an}$
300 - 360°	1	1	0	0	1	-1	$S_{bp} \& S_{cn}$

III CLOSED LOOP CONTROL

The overall block diagram is shown in Fig. 3. It consists of a current control loop which regulate the torque of the BLDC motor and a speed control loop that regulates the speed of the BLDC motor. The specification details of BLDC are shown in table 3. The set speed ω^* (rad/sec) and actual rotor speed ω_{actual} (rad/sec) of the motor are compared and the speed error ω_{error} is given to the PI speed controller. The regulation of speed is accomplished with speed controller and reference torque T_{ref} is produced. An anti-windup circuit is used to overcome the saturation in integral controller. The reference current (I_{ref}) is derived from the reference torque T_{ref} and it is used in the current control loop. Current control loop consists of reference current generator, PI current controller and PWM pulse generator.

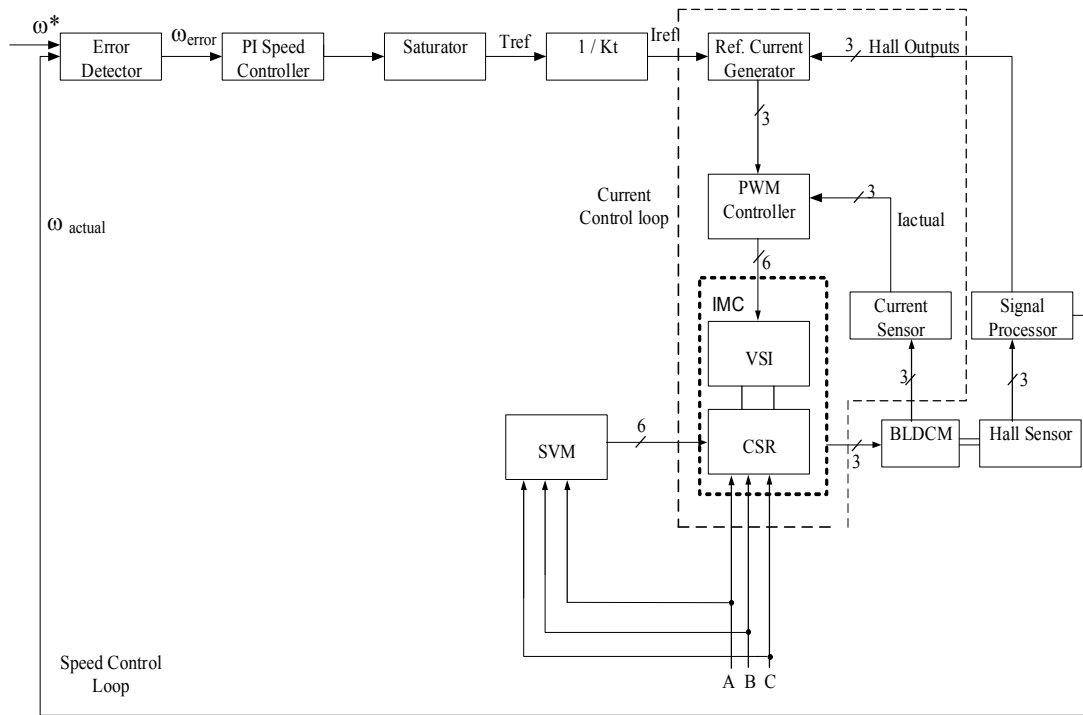


Figure 3. Block Diagram of closed loop control

The reference current generator block generates the three phase reference currents (I_{a^*} , I_{b^*} , I_{c^*}) which are timed according to the hall sensor and it is shown in Table 2. These appropriate timed reference currents are in rectangular shape and in phase with the respective trapezoidal back EMF to generate the maximum unidirectional torque. The PI current controller and PWM generator process the current error and generate the PWM pulses for the VSI. SVM technique is used for CSR. The K_p and K_i of speed and current controllers are tuned manually using Ziegler-Nichols method and the values are 0.07, 1.40 and 3 respectively. The K_p and K_i of speed and current controllers are also tuned using FFA for the torque ripple minimization and for the enhancement of input current. The K_p and K_i values of speed and current controller are 0.0612, 1.4685, 10 and 8.1355 respectively. The parameters used in FFA are shown in Table 4.

Table 3. Specification details of BLDC motor

Motor rating	1.1HP	Pole Pairs	2
Voltage	250 V	Speed	4600 RPM
Rated Current	4.52 A	Inertia	1.8 kgcm ²
Peak Current	13.5A	Stator Phase Resistance	3.07Ω
Rated Torque	2.2Nm	Stator Phase Inductance	6.57mH
Peak torque	6.6Nm		

Table 4. Parameters of FFA

Population of fireflies	25	Randomization parameter α	$\alpha_0 \delta$
Maximum attractiveness β_0	1	Initial Randomization parameter α_0	0.01L
Light absorption coefficient γ	$1/\sqrt{L}$	Cooling factor δ	0.96
Maximum Value of x_i^{max}	25	No. of iterations	100
Minimum Value of x_i^{min}	0	Number of dimension (Parameters)	4
Scaling factor $L (x_i^{max} - x_i^{min})$	25		

IV RESULTS& DISCUSSIONS

The input voltage of 124V is given to three phase IMC. Initially, the motor is started with no load and at the set speed of 500RPM. It is observed that the peak overshoot in speed is 507 RPM in FFA based system whereas it is 542 in manually based system and it is shown in fig. 4.

The load of 1 Nm is applied to the motor. The torque ripple in Ziegler-Nichols tuned system is 0.35 Nm and in FFA based system the torque ripple is 0.1 Nm which is lesser than that of prior one and it is shown in Fig. 5. Fig.6 shows the input current in both the systems and it is observed that, the input current is better in FFA based system. The simulation results are verified using the hardware setup. Figure 7 shows the three phase input current and virtual DC link voltage in FFA based system. Figure 8 shows the input voltage and current of BLDC motor and hardware setup. From the waveforms and table 5, it is observed that the torque ripple is minimized and input current waveform is improved in FFA tuned system compared to the Ziegler-Nichols tuned system.

Table 5. Performance Comparison of BLDCM using Ziegler-Nichols and FFA tuning methods

$T_L = 1 Nm$	PI (Ziegler-Nichols)	PI (FFA)
T_{max}	1.5	1.36
T_{min}	1.15	1.26
Ripple	0.35	0.1
Reduction in Speed (RPM)	Regains after 0.1 sec	Regains after 0.1 sec
Input Current	Sinusoidal (high harmonics)	Sinusoidal (less Harmonics)

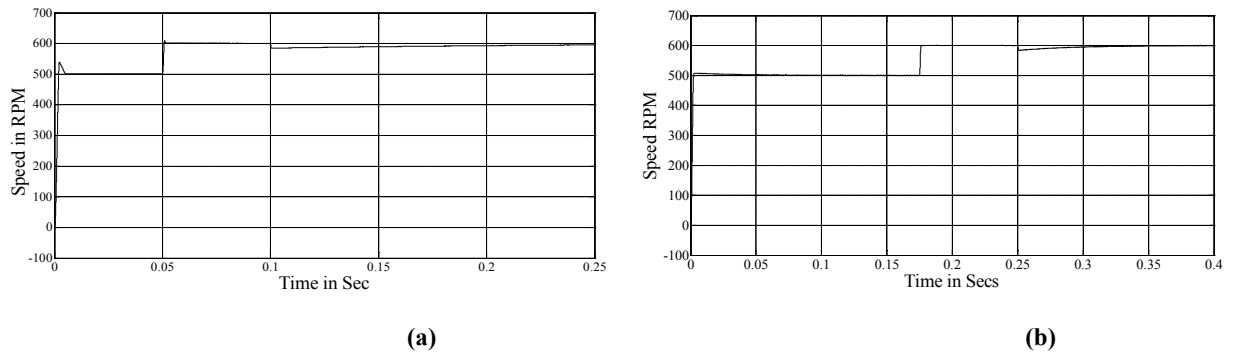


Figure. 4. Speed Characteristics in (a) Ziegler-Nichols tuned System (b) FFA based System

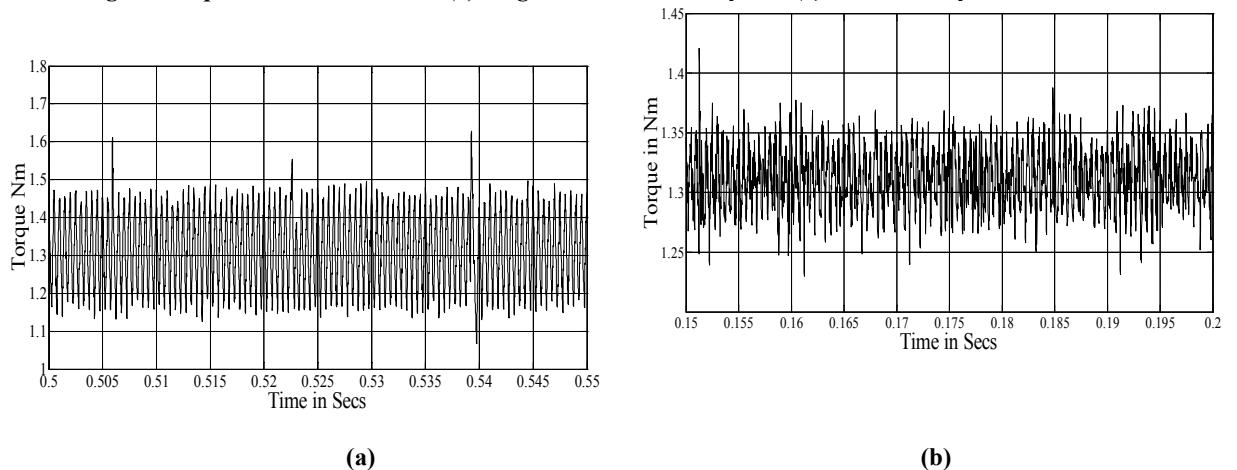


Figure. 5. Torque characteristics in (a) PI Ziegler-Nichols (b) PI FFA based system

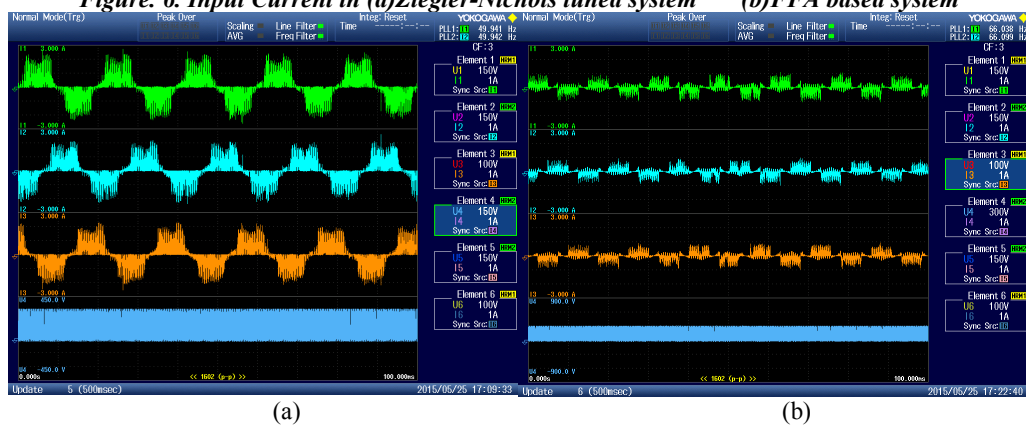
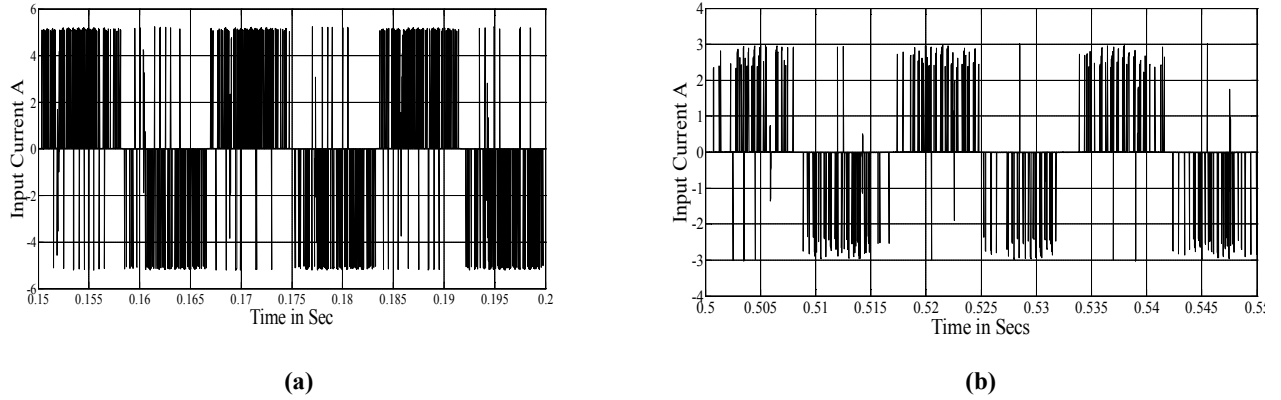


Figure 7. (a) Input current of IMC and virtual DC link voltage (b) Input current of BLDC motor

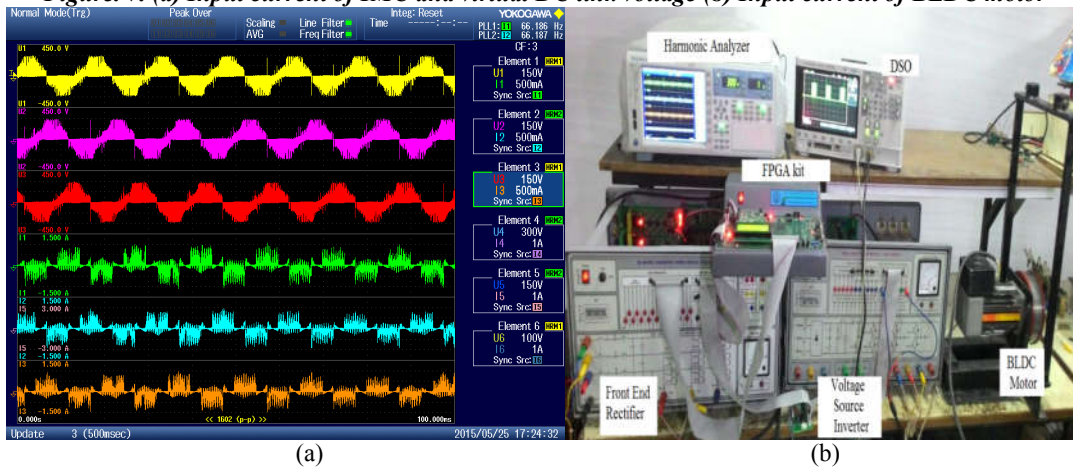


Figure 8 (a) Input voltage and current of BLDC motor

(b) Hardware setup

V. CONCLUSION

This paper presents indirect matrix converter fed BLDC motor. Since the IMC has no DC storage elements such as capacitors, the system guarantees a long life. Enhancement of input current and minimization torque ripple are achieved using the PI speed and PI torque controller. The proportional and integral gains of speed and torque controllers are tuned using Ziegler-Nichols tuning method. The gains are also tuned using one of the optimization methods known as firefly algorithm. The torque ripple, speed and input current of the system in both the methods are compared and contrasted in this paper. The simulation results are verified with the hardware results. It is concluded that the torque ripple is minimum and input current waveform is improved in FFA tuned system compared to Ziegler-Nichols tuned system.

REFERENCES

1. Mandel, Yoni, and George Weiss. "Adaptive internal model-based suppression of torque ripple in brushless DC motor drives." *Systems Science & Control Engineering*, vol. 3, no. 1, pp. 162-176, 2015.
2. WeizheQian; Panda, S.K.; Jian-XinXu Torque ripple minimization in PM synchronous motors using iterative learning control, *IEEE transaction on Power Electronics*, vol.19 , no.2, pp.272-279 , 2004
3. Zhang Xiaofeng& Lu Zhengyu, 'A New BLDC Motor Drives Method Based on BUCK Converter for Torque Ripple Reduction' , *Proceedings of the fifth International Power Electronics and Motion Control Conference*, vol. 2, pp. 1-4, 2006.
4. Wei Chen, Changliang Xia & Mei Xue , 'A Torque ripple suppression circuit for brushless DC motors based on power DC/DC converters', *Proceedings of the IEEE Conference on Industrial Electronics and Applications*, pp.1453-1457, 2008.
5. Tingna Shi, YuntaoGuo, Peng Song &Changliang Xia, 'A New Approach of Minimizing Commutation Torque Ripple for Brushless DC Motor Based on DC-DC Converter', *IEEE Transactions on Industrial Electronics*, vol. 57, no. 10, pp. 3483-3490, 2010.
6. Chuang, HS, Yu-Lung Ke& Chuang, YC, 'Analysis of commutation torque ripple using different PWM modes in BLDC motors', *Proceedings of the Technical Conference on Industrial & Commercial Power Systems*, pp.1-6, 2009.
7. Jiancheng Fang, Haitao Li &Bangcheng Han , 'Torque Ripple Reduction in BLDC Torque Motor With Nonideal Back EMF', *IEEE Transactions on Power Electronics*, vol. 27, no. 11, pp. 4630-4637, 2012.
8. Gao, Jin, and Yuwen Hu. "Direct self-control for BLDC motor drives based on three-dimensional coordinate system." *Industrial Electronics, IEEE Transactions on* 57.8 (2010): 2836-2844.
9. Fang, Jiancheng, Xinxu Zhou, and Gang Liu. "Instantaneous torque control of small inductance brushless DC motor." *Power Electronics, IEEE Transactions on* 27.12 (2012): 4952-4964.
10. Fang, Jiancheng, Xinxu Zhou, and Gang Liu. "Precise accelerated torque control for small inductance brushless DC motor." *Power Electronics, IEEE Transactions on* 28.3 (2013): 1400-1412.
11. Ibrahim, H. E. A., F. N. Hassan, and Anas O. Shomer. "Optimal PID control of a brushless DC motor using PSO and BF techniques." *Ain Shams Engineering Journal* 5.2 (2014): 391-398.
12. Bayoumi, E. H. E., and H. M. Soliman. "PID/PI tuning for minimal overshoot of permanent-magnet brushless DC motor drive using particle swarm optimization." *ELECTROMOTION-CLUJ NAPOCA-* 14.4 (2007): 198 - 208.
13. J. W. Kolar, F. Schafmeister, S. D. Round, and H. Ertl, Novel Three-Phase AC-AC Sparse Matrix Converters, *IEEE Trans. Power Electron.*, 22, 1649-1661, 2007.
14. Gruson, P. Le Mogne, P. Delarue, M. Arpillière, and X. Cimetiere, Comparison of Losses between Matrix and Indirect Matrix Converters with an Improved Modulation, *IEEE International Symposium Ind. Electron.* (2010) 718-723.
15. Faraji ,V, Agashi, M, Khaburi, D.A &Kalantar, M 2010,'Direct torque control with improved switching for induction motor drive system fed by indirect matrix converter, *National Conference on Electrical Electronics and Computer Engineering (ELECO)*, pp 309-314.
16. Karuvelam, P. Subha, and M. Rajaram. "Modified Firefly Algorithm For Selective Harmonic Elimination In Single Phase Matrix Converter." *International Journal of Applied Engineering Research* 9.23 (2014): 22325-22336.
17. Karuvelam, P. Subha, and M. Rajaram. "Matrix Converter Fed Brushless DC Motor Using Field Programmable Gate Array." *World Academy of Science, Engineering and Technology, International Journal of Electrical, Computer, Energetic, Electronic and Communication Engineering* 8.11 (2015): 1825-1832.
18. Karuvelam, P. Subha, and M. Rajaram. "Real time Implementation of SHE PWM in Single Phase Matrix Converter using Linearization Method." *Journal of Electrical Engineering and Technology* 10.4 (2015): 1682-1691.
19. Subha Karuvelam, P., and M. Rajaram. "A novel technique for real time implementation of SHE PWM in single phase matrix converter." *Tehnički vjesnik* 23.5 (2016): 1481-1488.